Small Molecule Therapeutics

Molecular Cancer Therapeutics

Antitumor Effects in Gastrointestinal Stromal Tumors Using Photodynamic Therapy with a Novel Glucose-Conjugated Chlorin

Mamoru Tanaka[1], Hiromi Kataoka[1], Shigenobu Yano[2,3], Hiromi Ohi[4], Kazuhiro Moriwaki[5], Haruo Akashi[5], Takahiro Taguchi[6], Noriyuki Hayashi[1], Shingo Hamano[1], Yoshinori Mori[1], Eiji Kubota[1], Satoshi Tanida[1], and Takashi Joh[1]

Abstract

Gastrointestinal stromal tumors (GIST) are the most common mesenchymal tumors of the gastrointestinal tract. Except for surgical resection, no effective treatment strategies have been established. Photodynamic therapy (PDT) consists of intravenous administration of a photosensitizer, activated by a specific wavelength of light, which produces reactive oxygen species that directly kill tumor cells. We analyzed the efficacy of PDT using a newly developed photosensitizer, 5,10,15,20-tetrakis [4-[β-D-glucopyranosylthio-2,3,5,6-tetrafluorophenyl]-2,3,[methano[*N*-methyl] iminomethano] chlorin (H_2TFPC-SGlc), for the GIST treatment. Various photosensitizers were administered *in vitro* to GIST (GIST-T1) and fibroblast (WI-38) cells, followed by irradiation, after which cell death was compared. We additionally established xenograft mouse models with GIST-T1 tumors and examined the accumulation and antitumor effects of these photosensitizers *in vivo*. *In vitro*, the expression of the glucose transporters GLUT1, GLUT3, and GLUT4, the cellular uptake of H_2TFPC-SGlc, and apoptosis mediated by PDT with H_2TFPC-SGlc were significantly higher in GIST-T1 than in WI-38 cells. *In vivo*, H_2TFPC-SGlc accumulation was higher in xenograft tumors of GIST-T1 cells than in the adjacent normal tissue, and tumor growth was significantly suppressed following PDT. PDT with novel H_2TFPC-SGlc is potentially useful for clinical applications about the treatment of GIST. *Mol Cancer Ther; 13(4); 767–75. ©2014 AACR.*

Introduction

Gastrointestinal stromal tumors (GIST) are the most common mesenchymal tumors of the digestive tract. GIST cells are believed to originate from either progenitors of the interstitial cells of Cajal (1, 2), a population of spindle-shaped cells that are the pacemaker cells of the gut, or from an interstitial mesenchymal precursor stem cell (3, 4). GISTs >2 cm in diameter are typically resected, whereas GISTs <2 cm in diameter are monitored closely for rapid growth or metastasis (5–7). As no effective treatments other than surgical resection are available, it is necessary to elucidate new therapies and approaches for the treatment of GISTs, particularly when they are small (8).

One such approach, photodynamic therapy (PDT), has several advantages over conventional cancer treatments. PDT consists of the intravenous administration of a photosensitizer, which preferentially localizes within the tumor, followed by activation with a specific wavelength of light (9). Activation of the photosensitizer causes the conversion of molecular oxygen into various reactive oxygen species (ROS) that directly induce the death of the tumor cells or damage the tumor-associated vasculature (10). PDT is relatively noninvasive and has a lower systemic toxicity because irradiation and activation occur only at the tumor site (10, 11). Thus, PDT has been widely used to treat various tumors, which can be directly reached by different wavelengths of light, such as lung, esophageal, gastric, breast, head and neck, bladder, and prostate cancer (9). Compared with other therapies, PDT often produces a high cure rate with a low recurrence rate (12). Photofrin, a first-generation photosensitizer, is widely used in the clinic (10, 11); however, talaporfin, a second-generation photosensitizer, has several advantages over photofrin, including decreased prolonged photosensitization (13). Talaporfin-mediated PDT has been examined in the treatment of several solid tumors (14, 15). However, the insufficiency of efficacy and skin photosensitivity

Authors' Affiliations: [1]Departments of Gastroenterology and Metabolism, Nagoya City University Graduate School of Medical Sciences, Nagoya; [2]Graduate School of Materials Science, Nara Institute of Science and Technology, Nara; [3]Office of Society-Academia Collaboration for Innovation, Kyoto University, Kyoto; [4]Division of Materials and Manufacturing Science, Osaka University, Osaka; [5]Research Institute of Natural Sciences, Okayama University of Science, Okayama; and [6]Division of Human Health and Medical Science, Graduate School of Kuroshio Science, Kochi University Nankoku, Kochi, Japan

Note: Supplementary data for this article are available at Molecular Cancer Therapeutics Online (http://mct.aacrjournals.org/).

Corresponding Author: Hiromi Kataoka, Department of Gastroenterology and Metabolism, Nagoya City University Graduate School of Medical Sciences, 1 Kawasumi, Mizuho-cho, Mizuho-ku, Nagoya 467-8601, Japan. Phone: 81-52-853-8211; Fax: 81-52-852-0952; E-mail: hkataoka@med.nagoya-cu.ac.jp

doi: 10.1158/1535-7163.MCT-13-0393

remains unsolved, so the more effective photosensitizer is expected to be developed.

In this study, we evaluated the efficacy of PDT with a new glucose-conjugated photosensitizer, glycoconjugated chlorin(5,10,15,20-tetrakis [4-[β-D-glucopyranosylthio- 2,3,5,6-tetrafluorophenyl]-2,3,[methano[*N*-methyl] iminomethano] chlorin, H_2TFPC-SGlc) for the treatment of GIST *in vitro* and *in vivo*. As GIST cells readily take up glucose in positron emission tomography scans, and the long wavelengths of the light spectrum (red, 630–670 nm) can penetrate to the deep layers of the stomach wall, PDT consisting of the administration of H_2TFPC-SGlc with activation at 660 nm is a good candidate for GIST treatment. In our previous study, we indicated that H_2TFPC-SGlc was able to induce apoptosis via singlet oxygen, was approximately 30 times more cytotoxic than talaporfin during PDT, and could be a potential photosensitizer of PDT of gastric and colon cancer *in vitro* and *in vivo* as we believe that it has superior cancer cell selectivity and specificity (16).

Therefore, in this study, we evaluated the efficacy of PDT with a new photosensitizer—glucose-conjugated chlorin (H_2TFPC-SGlc)—for the treatment of GIST *in vitro* and *in vivo*.

Materials and Methods

Photosensitizers

5,10,15,20-tetrakis(pentafluorophenyl)-2,3-(methano[*N*-methyl]iminomethano])chlorin) (H_2TFPC) and H_2TFPC-SGlc (Fig. 1A) were synthesized and provided by the laboratory of the Kyoto University (Japan) and Okayama University of Science (Japan). They contain no isomers, based on 1H-NMR and 19F-NMR measurements (Supplementary Data S1).

Cell culture

The GIST-T1 cell line has been characterized in detail and was provided on July 14, 2011 by Taguchi and colleagues (17). WI-38 cells (Japanese Cancer Research Resources Bank, No. IFO50075), which are human embryonic fibroblasts derived from the lung, were cultured in Eagle minimum essential medium (Wako. Pure Chemical Industries Co. Ltd.) supplemented with 10% FBS and 1% ampicillin and streptomycin under 5% CO_2 at 37°C. The human GIST cell line, GIST-T1, was cultured in normal (1,000 mg/L) or high (4,500 mg/L) glucose Dulbecco's Modified Eagle Medium (Wako Pure Chemical Industries Co. Ltd.) supplemented with 10% FBS and 1% ampicillin and streptomycin under 5% CO_2 at 37°C (Fig. 1B).

Western blotting

Cells were washed with PBS (Sigma) 3 times and dissolved in 1 mL of cell lysis buffer (Cell Signaling Technology) containing 20 mmol/L Tris-HCl (pH 7.5), 150 mmol/L NaCl, 1 mmol/L Na_2EDTA, 1 mmol/L EGTA, 1% Triton, 2.5 mmol/L sodium pyrophosphate, 1 mmol/L β-glycerophosphate, 1 mmol/L Na_3VO_4, and 1 μg/mL leupeptin. One millimolar phenylmethylsulfonyl fluoride was added directly before use. Cells were disrupted for

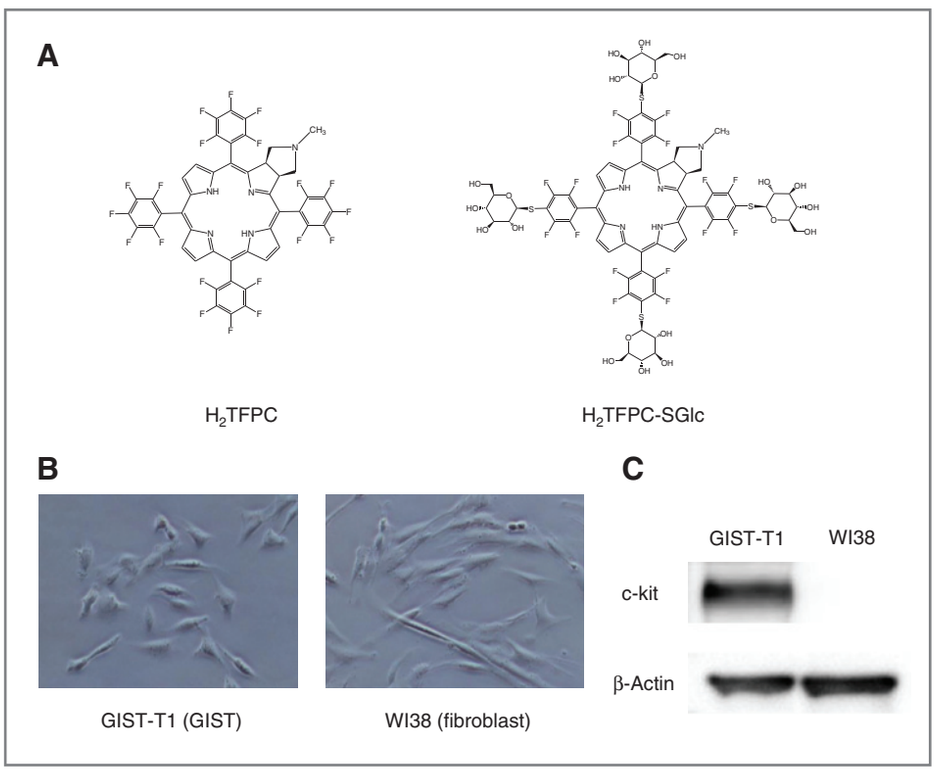

Figure 1. Chemical structure of photosensitizers and characteristics of cell lines. A, the structures of 5,10,15,20-tetrakis (pentafluorophenyl)-2,3-(methano[*N*-methyl]iminomethano) chlorin(H_2TFPC, left) and 5,10,15,20-tetrakis(4-(β-D-glucopyranosylthio)-2,3,5,6-tetrafluorophenyl)-2, 3-(methano[*N*-methyl] iminomethano) chlorin (H_2TFPC-SGlc, right) are shown. B, the morphologies of GIST-T1 and WI-38 cells were determined by microscopy. (magnification, ×200). C, c-Kit expression of GIST-T1 and WI-38 cells was investigated at the protein level by Western blotting. β-Actin was used as a loading control.

15 seconds on ice using a Bio-ruptor sonicator (Cosmo Bio) and centrifuged at 15,000 rpm for 10 minutes at 4°C. Each sample was normalized to an equal protein concentration using a Protein Assay Kit (Bio-Rad Laboratories). An equal quantity of 2× SDS-PAGE sample buffer [0.5 M Tris-HCl (pH 7.2), 1% SDS, 100 mmol/L β-mercaptoethanol, and 0.01% bromophenol blue] was added to each sample, and samples were boiled for 5 minutes at 100°C. Aliquots of each sample were separated by SDS-PAGE on an 8% to 15% gel and transferred on to a nitrocellulose membrane. The membrane was blocked with 5% skim milk in PBS for 1 hour at room temperature, followed by incubation with the primary antibodies anti-GLUT1, anti-GLUT3, or anti-GLUT4 (Santa Cruz Biotechnology, Inc., 1:2,000) overnight at 4°C. The membrane was washed with 0.05% Tween 20 in PBS 3 times at 5 minutes intervals, incubated with secondary antibody for 1 hours at room temperature, and washed again with 0.05% Tween 20 in PBS 3 times at 5-minute intervals. The membrane was incubated with enhanced chemiluminescence detection reagents (Amersham) for 1 minute at room temperature and exposed to scientific imaging film (Eastman Kodak). The proteins were visualized as dark bands. The membranes were stripped and reprobed with monoclonal β-actin antibody (Abcam) as an internal control.

Real-time reverse transcription PCR

GLUT1, *GLUT3*, *GLUT4*, and *GADPH* mRNA expression in GIST-T1 and WI-38 cells was measured by real-time reverse transcription PCR (RT-PCR). *GADPH* was chosen as an endogenous control to normalize the expression data. mRNA was reverse transcribed into complementary DNA (cDNA) using a high-capacity cDNA Reverse Transcription Kit (Applied Biosystems) according to the manufacturer's instructions. TaqMan Gene Expression Assays for *GLUT1* (Hs00892681_m1), *GLUT3* (Hs00359840_m1), *GLUT4* (Hs00168966_m1), and *GADPH* (Hs99999905_m1) were purchased from Applied Biosystems, and real-time quantitative RT-PCR analyses were performed in triplicate using an ABI 7500 Fast Real-Time PCR system (Applied Biosystems) according to the supplier's recommendations. All data are presented as fold change of internal control, and the results between cells were analyzed by the Welch *t* test.

Flow cytometry analysis

2-(N-[7-nitrobenz-2-oxa-1,3-diazol-4-yl]amino)-2-deoxy-D-glucose (2-NBDG; Peptide Institute, Osaka, Japan) is a widely used fluorescent tracer for monitoring D-glucose uptake into single living cells (18). To monitor the uptake of 2-NBDG, H_2TFPC, or H_2TFPC-SGlc into GIST-T1 or WI-38 cells, the cells were incubated with 2-NBDG, H_2TFPC, or H_2TFPC-SGlc for 0, 15, 30, 60, 120, or 240 minutes and washed once with PBS. 2-NBDG, H_2TFPC, and H_2TFPC-SGlc accumulation in the cells was measured using a FACSCalibur flow cytometer (BD Biosciences).

Cells were harvested from their plates using 0.25% trypsin-EDTA (GIBCO) and incubated with FITC-labeled active caspase-3 antibody (BD Biosciences) at 4°C for 30 minutes in the dark. Cells were neutralized with binding buffer and apoptotic cells were analyzed using a FACSCanto II Analyzer (BD Biosciences). Analyses were performed at 0, 1, 2, 4, 8, 12, 16, 20, and 24 hours after exposure.

At least 10,000 events were collected for each sample. The results between cells were analyzed by the Welch *t* test.

Intracellular localization

Cells were incubated with H_2TFPC (1 μmol/L, 20 μmol/L) or H_2TFPC-SGlc (1 μmol/L) at 4 hours and stained with organelle-specific fluorescent probes. Lysosomes were labeled with 0.1 μmol/L LysoTracker Green (Invitrogen) for 30 minutes at 37°C. Mitochondria were labeled with 0.1 μmol/L MitoTracker Green FM (Invitrogen) at 37°C for 10 minutes. Golgi bodies were labeled with 5 μmol/L NBD C6-ceramide at 4°C for 30 minutes. The endoplasmic reticulum was labeled with 0.1 μmol/L ER-Tracker Green (Invitrogen) at 37°C for 30 minutes. Stained cells were observed with a confocal laser microscope (Nikon A1 confocal system; Nikon Instech Co., Ltd.), and data were analyzed using NIS element imaging software (Nikon). Bandpass emission filters of 505 to 530 nm and 650 nm were used.

In vitro PDT

GIST-T1 and WI-38 cells were incubated with H_2TFPC or H_2TFPC-SGlc in cell culture medium for 4 hours. Cells were washed once with PBS, covered with PBS, and irradiated with of LED light (OptoCode Corporation) at 660 nm. Following irradiation, the PBS in the wells was exchanged for medium supplemented with 2% FBS, and the cells were incubated for the specified times before analyses. The results between cells were analyzed by the Welch *t* test.

Cell viability assay

Cell viability was analyzed by the WST-8 cell-proliferation assay. GIST-T1 and WI38 cells were seeded into 96-well culture plates at a concentration of 5×10^3 cells/100 μL/well and incubated overnight. Cells were incubated with H_2TFPC or H_2TFPC-SGlc at 37°C for 4 hours, irradiated, and further incubated for 24 hours. To determine survival, cells were incubated with the Cell Counting Kit-8 (Dojindo) according to manufacturer's protocol for 4 hours, and the absorption at 450 nm was measured with a microplate spectrophotometer (SPECTRA MAX340; Molecular Devices). Cell viability was expressed as a percentage of untreated control cells. The results between cells were analyzed by the Welch *t* test.

Animals and tumor models

Pathogen-free female nude mice (BALB/c Slc-nu/nu), 6 to 8 weeks of age, with a body weight of 20 to 25 g, were obtained from Japan SLC. Xenograft tumor models were established by subcutaneously implanting 5×10^6

GIST-T1 cells in 200 μL of PBS. The procedures in these experiments were approved by Nagoya City University Center for Experimental Animal Science, and mice were cared for according to the guidelines of the Nagoya City University for Animal Experiments.

Spectrophotometric analysis device

We examined the accumulation of H_2TFPC and H_2TFPC-SGlc in the xenograft tumor model using a semiconductor laser with a VLD-M1 spectrometer (M&M Co., Ltd.) that exposed a laser light with a peak wavelength of 405 ± 1 nm and a light output of 140 mW. The spectrometer and its accessory software (BW-Spec V3.24; B&W TEK, Inc.) were used to analyze the spectrum waveform, which revealed an amplitude peak (relative fluorescence intensity) of 505 nm for autofluorescence and 655 nm for H_2TFPC-SGlc. To reduce measurement error, we compared the relative fluorescence intensity ratios of H_2TFPC-SGlc in the target tissues, which were calculated by dividing the relative fluorescence intensity by that of autofluorescence. The results from the tumor and adjacent normal tissue were compared by the Welch *t* test.

In vivo PDT

Mice were administered H_2TFPC or H_2TFPC-SGlc by tail vein injection at a dose of 1.25 μmol/kg. Four hours after injection, the tumors were irradiated with 660 nm LED light (OptoCode Corporation) at a dose of 40 J/cm^2 (intensity: 49 mW/cm^2) to the skin directly above the tumor. Treatment was repeated 4 times at 10, 17, 24, and 31 days after tumor inoculation. Tumor growth was monitored daily by measuring the tumor volume with vernier calipers, and the tumor volume was calculated by the formula length × width × depth/2. The results were analyzed by the Bonferroni–Holm method to assess differences between groups.

Statistical analysis

Descriptive statistics and simple analyses were performed using the statistical package R, version 2.4.1 (www.r-project.org/). In all analyses, *P*-values < 0.05 were considered statistically significant.

Results

A GIST cell line, GIST-T1, expresses c-Kit

The GIST-T1 cell line was strongly positive for c-Kit, but the fibroblast cell line WI-38 was not, as shown in Fig. 1C. The expression of c-Kit has emerged as the most important defining feature of GIST and probably the gold standard for diagnosing GIST (19).

Expression of glucose transporters in cell lines

Expression of glucose transporters in these cells depends on the extracellular glucose concentration. We analyzed the expression of GLUT1, GLUT3, and GLUT4 protein and mRNA in GIST-T1 and WI-38 cells using Western blot analysis and RT-PCR analysis. GLUT1, GLUT3, and GLUT4 protein and mRNA expression increased significantly in GIST-T1 and WI-38 cells when cultured in normal glucose medium compared with high glucose medium. GIST-T1 cells significantly expressed higher GLUT1, GLUT3, and GLUT4 protein and mRNA than WI-38 cells in both normal and high glucose culture conditions (Fig. 2).

Cellular uptake of 2-NBDG, H_2TFPC, and H_2TFPC-SGlc

We first examined the uptake of 2-NBDG, H_2TFPC, and H_2TFPC-*SGlc in vitro* using GIST-T1 and WI-38 cells. Cells were incubated with 1 μmol/L 2-NBDG, H_2TFPC, or H_2TFPC-SGlc in normal or high glucose medium for the indicated times, and uptake was estimated by measuring the intensity of the characteristic red fluorescence at the single cell level using FACS. As shown in Fig. 3A (normal glucose medium) and 3B (high glucose medium), the uptake of 2-NBDG and H_2TFPC-SGlc was higher in GIST-T1 than in WI-38 cells. There was no apparent difference in the uptake of H_2TFPC between GIST-T1 and WI-38 cells. These results indicated that glucose conjugation to chlorin induced greater GIST cell specificity and selectivity. We tried to culture GIST-T1 cells in non-glucose medium, but GIST-T1 cells did not grow for a week in non-glucose medium. GIST-T1 cells in non-glucose medium for 4 hours did not change the uptake of H_2TFPC-SGlc from in normal glucose medium (Supplementary Fig. S1).

Subcellular localization of H_2TFPC-SGlc

Next, we investigated the subcellular localization of H_2TFPC-SGlc using fluorescence probes for intracellular organelles. Cells were loaded with H_2TFPC-SGlc and incubated with MitoTracker Green, LysoTracker Green, NBD C6-ceramide Green, or ER-Tracker Green to label the mitochondria, lysosomes, Golgi bodies, or endoplasmic reticulum, respectively. H_2TFPC-SGlc colocalized with MitoTracker and ER-Tracker, indicating that the photosensitizer accumulated in the mitochondria and endoplasmic reticulum (Fig. 3C). In addition, we also examined the subcellular localization of H_2TFPC. The expression level was low at 1 μmol/L, but H_2TFPC (20 μmol/L) was also mainly accumulated in the mitochondria and endoplasmic reticulum (Supplementary Fig. S2). These things suggested that chlorin (H_2TFPC) tends to be localized in the mitochondria and endoplasmic reticulum regardless of the conjugation of glucose.

PDT with H_2TFPC-SGlc induced cell death through apoptosis

We examined PDT-induced cell death with H_2TFPC and H_2TFPC-SGlc in normal (Fig. 4A) and high glucose medium (Fig. 4B). GIST-T1 and WI-38 cells were incubated with H_2TFPC and H_2TFPC-SGlc for 4 hours and irradiated with 16 J/cm^2 of 660 nm LED light. PDT with H_2TFPC-SGlc displayed significantly stronger toxicity than PDT with H_2TFPC and induced cell death more efficiently in GIST-T1 compared with WI-38 cells. The cytotoxicity of PDT with H_2TFPC-SGlc in GIST-T1 cells increased with increasing light doses in normal (Fig. 4C) and high glucose medium (Fig. 4D). There was no apparent difference in

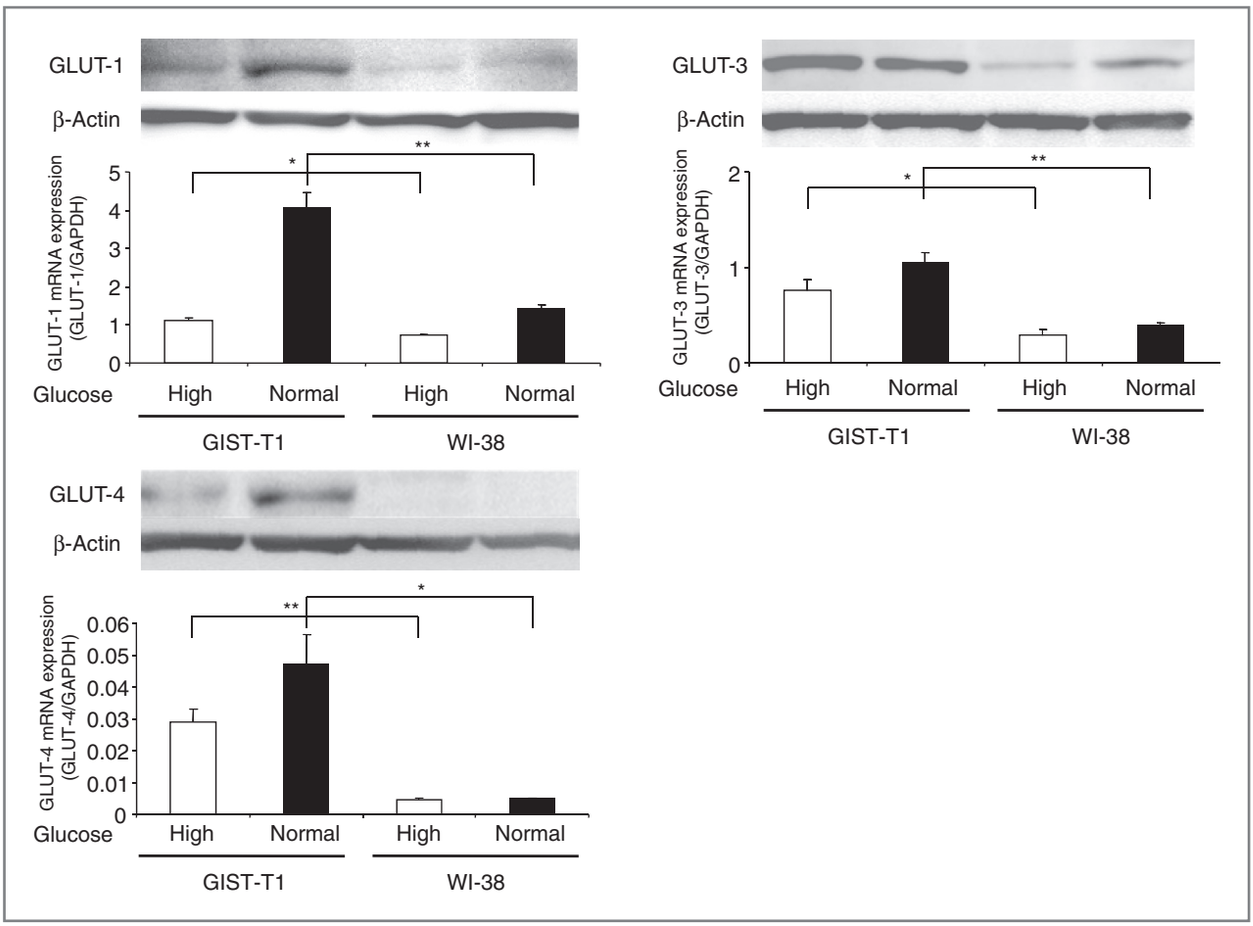

Figure 2. Expression of glucose transporters in cell lines. GLUT1, GLUT3, and GULT4 protein and mRNA expression levels in GIST-T1 and WI-38 cells were evaluated in normal or high glucose medium. Data are means of 3 independent experiments ± SE. **, $P < 0.01$; *, $P < 0.05$.

toxicity between the normal and high glucose medium. We also measured the mean fluorescence intensity of active caspase-3 by FACS as a marker for apoptosis. Mean fluorescence intensity increased at 4 hours after irradiation and peaked at 16 hours. H_2TFPC-SGlc–mediated PDT induced apoptosis more efficiently in GIST-T1 than in WI-38 cells. There was no detectable difference in apoptosis induction between normal (Fig. 4E) and high glucose media (Fig. 4F).

Accumulation of H_2TFPC-SGlc in GIST tumors

We examined the ability of H_2TFPC-SGlc to accumulate in xenograft GIST tumors established by subcutaneously implanting GIST-1 cells. Following tail vein injection of either 1.25 μmol/kg H_2TFPC or H_2TFPC-SGlc, the spectrum waveform from the xenograft tumors was analyzed by a VLD-M1 spectrophotometer. The spectrum waveform showed 2 peaks of fluorescence emission spectra, one at 505 nm, corresponding to autofluorescence, and one at 655 nm, corresponding to either H_2TFPC or H_2TFPC-SGlc. We then measured the relative fluorescence intensity ratio of H_2TFPC or H_2TFPC-SGlc in the tumors and the adjacent normal tissue. The relative fluorescence intensity ratio of H_2TFPC-SGlc was highest 4 hours after drug administration. H_2TFPC-SGlc accumulated in the tumor tissue at a significantly higher rate than in the adjacent normal tissue, but H_2TFPC did not (Fig. 5A). Furthermore, we measured the biodistribution of H_2TFPC and H_2TFPC-SGlc in xenograft models by using spectrophotometer. Significant accumulation of H_2TFPC-SGlc to the tumor tissue was detected. Among the organ tissues, H_2TFPC-SGlc tends to accumulate in liver and kidney, but these accumulations were much lower than that in tumor (Supplementary Data S2).

Antitumor effects of H_2TFPC-SGlc *in vivo*

To determine the antitumor effects of H_2TFPC-SGlc on xenograft tumors in mice, mice were administered H_2TFPC or H_2TFPC-SGlc at a dose of 1.25 μmol/kg by i.v. 10 days after tumor inoculation and then irradiated with 660 nm LED light at 40 J/cm^2. The tumor sizes before irradiation were 20 to 50 mm^3. H_2TFPC-SGlc–mediated PDT was repeated every 7 days for 4 cycles. Analysis determined that there was damage to the tumor without damage to the adjacent normal tissues. H_2TFPC-SGlc–mediated PDT ($n = 5$) suppressed tumor growth significantly

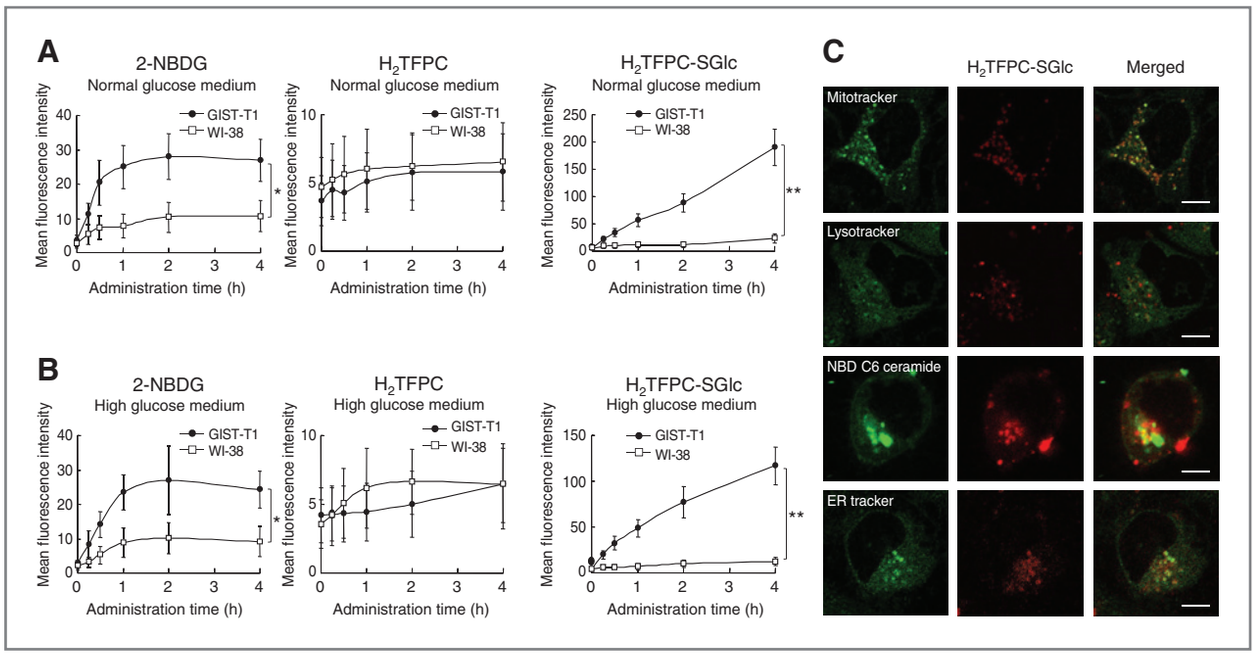

Figure 3. Uptake and subcellular localization of H_2TFPC-SGlc. A and B, GIST-T1 and WI-38 cells were incubated in normal (A) or high (B) glucose medium with 1 μmol/L of glucose (2-NBDG), H_2TFPC, or H_2TFPC-SGlc for various timepoints, and the uptake of the drugs was estimated by FACS. Data are the mean fluorescence intensity ± SE. **, $P < 0.01$; *, $P < 0.05$. C, GIST-T1 cells were loaded with H_2TFPC-SGlc (1 μmol/L) for 4 hours and labeled with MitoTracker Green, LysoTracker Green, NBD-C6 ceramide Green or ER-Tracker Green. The images were obtained by confocal microscopy (original magnification ×1,000; scale bar, 10 μm).

compared with the control treatment (light alone) and H_2TFPC-mediated PDT ($P < 0.01$; Fig. 5B). The treatments had no obvious side effects, such as diarrhea and/or weight loss (data not shown). Single H_2TFPC-SGlc–mediated PDT also significantly suppressed tumor growth ($P < 0.01$; Supplementary Fig. S3).

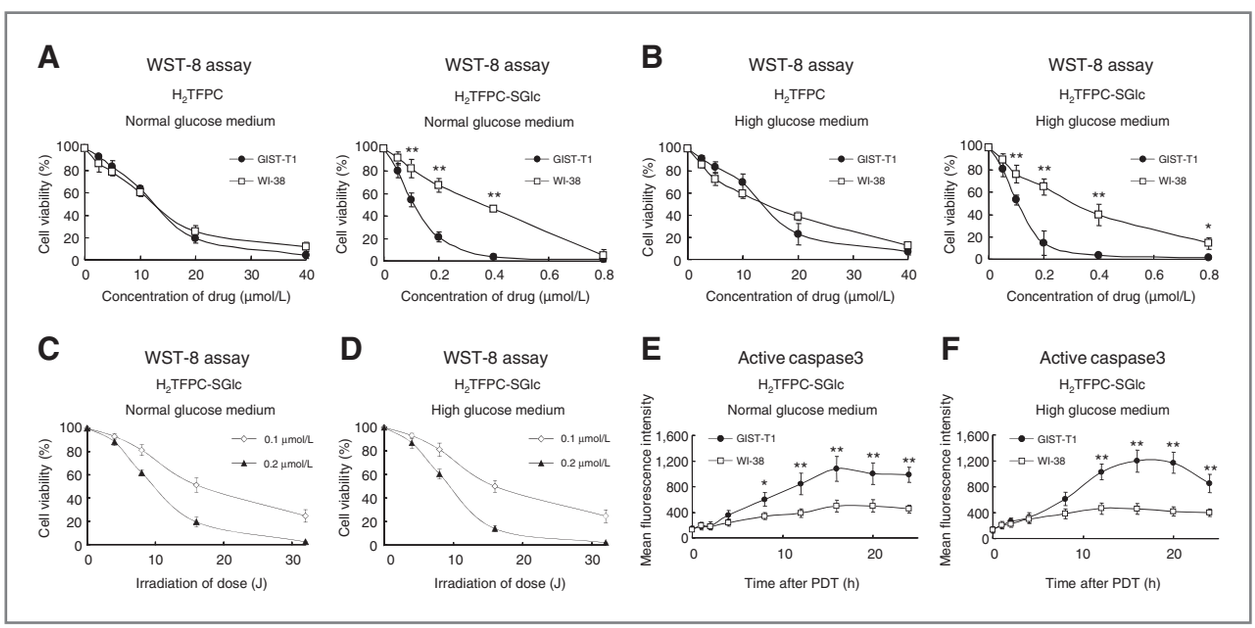

Figure 4. Cell death by PDT. A–D, GIST-T1 and WI-38 cells were incubated in normal (A) or high (B) glucose medium with various concentrations of H_2TFPC or H_2TFPC-SGlc, irradiated with 16 J/cm^2 of 660 nm LED light, and incubated for 24 hours. GIST-T1 cells in normal (C) or high (D) glucose medium were incubated with 0.1 or 0.2 μmol/L of H_2TFPC-SGlc and irradiated with various doses of 660 nm LED light. Cell viability was determined by a WST-8 assay. Data are means of 3 independent experiments ± SE. **, $P < 0.01$; *, $P < 0.05$. E and F, GIST-T1 or WI-38 cells in normal (E) or high (F) glucose medium were incubated with 1 μmol/L of H_2TFPC-SGlc, irradiated with 16 J/cm^2 of 660 nm LED light, and incubated for various lengths of time. Cells were stained with FITC-labeled active caspase-3 antibody, and apoptosis was analyzed through FACS. Data are means of 3 independent experiments ± SE. **, $P < 0.01$; *, $P < 0.05$.

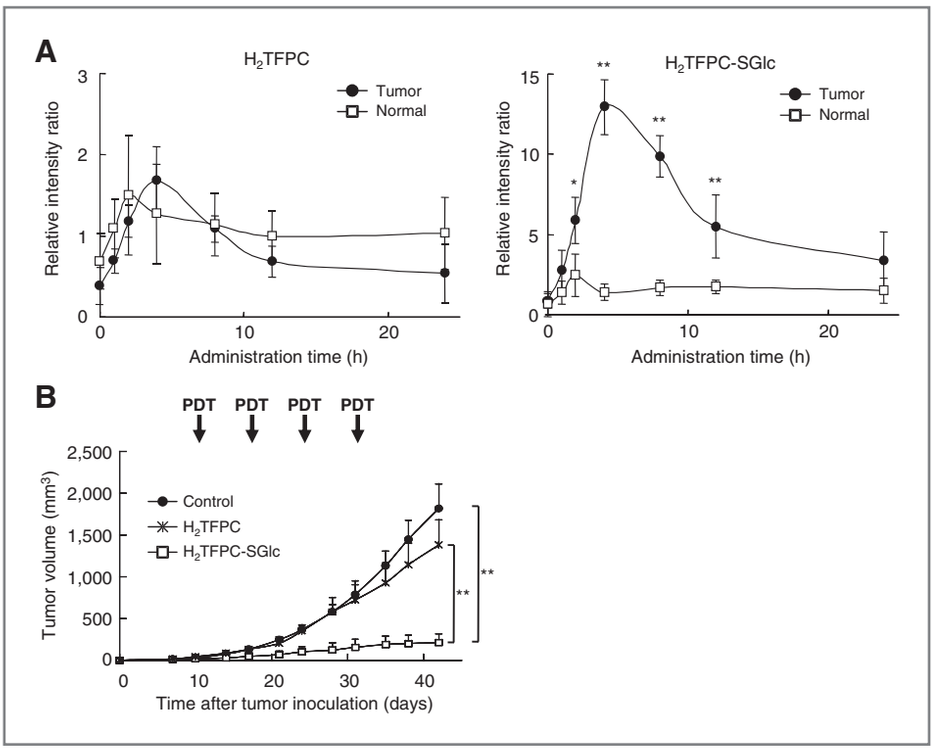

Figure 5. Accumulation in tumors and inhibition of tumor growth by PDT. GIST cells were inoculated in the dorsal skin of mice at a concentration of 5×10^6 cells/200 μL in PBS. H_2TFPC or H_2TFPC-SGlc at a concentration of 1.25 μmol/kg was administered by tail vein injection into tumor-bearing mice. A, the relative intensity of H_2TFPC or H_2TFPC-SGlc and autofluorescence were measured using a spectrometer at various timepoints after injection. The relative fluorescence intensity ratio in the tumor or adjacent normal tissue was calculated by dividing the relative fluorescence intensity of photosensitizers by that of autofluorescence. Data are means ± SE ($n = 5$ for H_2TFPC and $n = 5$ for H_2TFPC-SGlc). **, $P < 0.01$; *, $P < 0.05$. B, mice were irradiated with 40 J/cm^2 of LED light at 660 nm 4 hours after injection. Treatment was repeated 4 times at 10, 17, 24, and 31 days after tumor inoculation. Tumor volumes were monitored for 42 days total. Data are means ± SE ($n = 5$ for H_2TFPC and $n = 5$ for H_2TFPC-SGlc). **, $P < 0.01$.

Discussion

H_2TFPC-SGlc, a chlorin-based photosensitizer, was expected to have a number of advantages in PDT, including significant reductions in dark cytotoxicity, improved water-solubility, greater cellular uptake, and sugar-dependent photocytoxicity over currently used photosensitizers (20–22). In a previous study, we have reported that H_2TFPC-SGlc was 30 times more cytotoxic to gastric cancer cells *in vitro* as compared with the second-generation photosensitizer, talaporfin. Moreover, in xenograft tumors, H_2TFPC-SGlc accumulation was higher and significantly suppressed tumor growth as compared with talaporfin (16).

In this study, we investigated whether H_2TFPC-SGlc could act as a potential photosensitizer of PDT in GIST *in vitro* and *in vivo*. *In vitro*, H_2TFPC-SGlc–mediated PDT was shown to induce cell death via apoptosis. *In vivo*, H_2TFPC-SGlc–mediated PDT suppressed tumor growth and produced no observable adverse effects on normal adjacent tissues. These results indicate that PDT with H_2TFPC-SGlc is a minimally invasive therapeutic modality for clinical treatment of GIST. We used the GIST-T1 cell line, which was established from a patient with metastatic GIST by Taguchi and colleagues (17). GIST-T1 cell line expresses c-Kit oncogene and is considered to be one of the most representative GIST cell lines that mimic the nature of human GIST. In addition, GIST-T1 is the only cell line that can be used for a xenograft model *in vivo* at this point (Fig. 1C).

There have been many attempts to develop new photosensitizers that show preferential accumulation within the target tumor tissue through conjugation with various active targeting approaches, such as conjugation with peptides or antibodies (23–25), incorporation within liposomes (26, 27), and encapsulation within polymeric nanoparticles (28–31). To initiate accumulation in the target tumor, H_2TFPC-SGlc was developed by linking glucose to the photosensitizer chlorin. *In vitro*, the uptake of H_2TFPC-SGlc in GIST-T1 cells was much greater than that in normal WI-38 cells. The uptake of 2-NBDG was also significantly higher in GIST-T1 cells than in WI-38 cells; however, there was no changes in H_2TFPC uptake between GIST-T1 and WI-38 cells (Fig. 3A and B). *In vivo*, H_2TFPC-SGlc significantly accumulated to a greater extent in the tumor tissue than in the adjacent normal tissue (Fig. 5A). These results indicate that the linkage of glucose may be a useful tool for drug delivery in GIST-T1 as well as gastric cancer cells.

GLUT1 is believed to maintain basal glucose transport in most cell types (32–34) and seems to be the predominant

glucose transporter in many types of cancer cells, although the expressions of GLUT2, GLUT3, and GULT4 have been detected in cancer cells by immunohistochemistry or RNA analysis (34–37). We tried to examine the role of GLUT in H_2TFPC-SGlc uptake by knockdown of GLUT1, 2, and 4. However, knockdown of GLUT1, 2, and/or 4 did not change the uptake of H_2TFPC-SGlc. We speculate that GLUT2 and/or GLUT4 substitutes under silencing GLUT1, and vice versa. GLUT1 expression often correlates with the ability to detect tumors by positron emission tomography (38–40). Rapid uptake of glucose (as evidenced by positron emission tomography) in GIST typically associated with KIT mutations and increased cell survival (41). In colon cancer, GLUT1 expression is recently speculated to be the most frequently increased transcripts with the KRAS and BRAF mutation (42). In gastric cancer, GLUT1 has been reported to be expressed during gastric carcinogenesis (43, 44) and very recently gastric cancers with microsatellite instability exhibit high fluorodeoxyglucose uptake on positron emission tomography (45). Because the expressions of GLUT1, GLUT3, and GULT4 in GIST-T1 cells were significantly higher than those in WI-38 cells, these 3 glucose transporters may play crucial roles in the cellular uptake of H_2TFPC-SGlc into GIST-T1 cells (Fig. 2).

Intense research has been performed to identify the molecular functions that regulate the crosstalk between apoptosis and the other major cell death subroutines (e.g., necrosis and autophagic cell death). The function of the necrotic pathway was initiated by endoplasmic reticulum/Golgi body photodamage, the apoptotic pathway by mitochondrial photodamage, and the autophagic pathway by endoplasmic reticulum photodamage (46). We observed that PDT with H_2TFPC-SGlc induced apoptotic cell death in GIST cells (Fig. 4E and F). As shown in Fig. 3C, H_2TFPC-SGlc accumulated in mitochondria and the endoplasmic reticulum. It remains a possibility that PDT with H_2TFPC-SGlc induces cell death by necrosis and/or autophagy.

Previous PDT experiments with the photosensitizers photofrin and/or talaporfin used irradiation doses of >100 J/cm^2 in carcinoma xenografts models (47–49). In our study, H_2TFPC-SGlc–mediated PDT showed antitumor effects *in vitro* and *in vivo* with a relatively low irradiation dose of 40 J/cm^2. This indicated that the high cancer cell selectivity and specificity of H_2TFPC-SGlc could reduce the total energy of light irradiation needed in H_2TFPC-SGlc–mediated PDT. This reduction may further reduce the side effects related to the damage of adjacent normal tissue.

As chemotherapy and/or radiation therapy are not solely effective for GIST treatment, novel treatments for GIST have been explored. In this study, we conclude that H_2TFPC-SGlc–mediated PDT had specificity for GIST-T1 cells and effectively suppressed the growth of xenograft tumors through apoptosis without observable damage to the adjacent normal tissue. Based on the properties and characteristics of H_2TFPC-SGlc presented in this study, we suggest that H_2TFPC-SGlc is a potential photosensitizer for PDT of GIST.

Disclosure of Potential Conflicts of Interest

No potential conflicts of interest were disclosed.

Authors' Contributions

Conception and design: M. Tanaka, H. Kataoka, S. Yano
Development of methodology: M. Tanaka, H. Kataoka, S. Yano, S. Hamano, E. Kubota
Acquisition of data (provided animals, acquired and managed patients, provided facilities, etc.): M. Tanaka, H. Ohi, S. Hamano, E. Kubota
Analysis and interpretation of data (e.g., statistical analysis, biostatistics, computational analysis): M. Tanaka, Y. Mori
Writing, review, and/or revision of the manuscript: M. Tanaka, H. Kataoka, S. Yano
Administrative, technical, or material support (i.e., reporting or organizing data, constructing databases): S. Yano, K. Moriwaki, H. Akashi, T. Taguchi, N. Hayashi, Y. Mori, E. Kubota, S. Tanida
Study supervision: H. Kataoka, S. Yano, H. Akashi, T. Joh

Acknowledgments

The authors thank Y. Ito and C. Koike at Nagoya City University Graduate School of Medical Sciences for technical assistance.

Grant Support

This work was financially supported by JSPS KAKENHI Grant Number 23590923, JSPS KAKENHI Grant Number 24790717, JSPS KAKENHI Grant Number 25288028, the Japan-German exchange program supported by the JSPS and the Deutsche Forschungsgemeinschaft, the Hori sciences and arts foundation (2013), Japan Science and Technology Agency A-step (2011), The Japanese Foundation For Research and Promotion of Endoscopy (2009), and the Aichi Cancer Research Foundation (2013).

The costs of publication of this article were defrayed in part by the payment of page charges. This article must therefore be hereby marked *advertisement* in accordance with 18 U.S.C. Section 1734 solely to indicate this fact.

Received May 16, 2013; revised January 10, 2014; accepted February 11, 2014; published OnlineFirst February 19, 2014.

References

1. Perez-Atayde AR, Shamberger RC, Kozakewich HW. Neuroectodermal differentiation of the gastrointestinal tumors in the Carney triad. An ultrastructural and immunohistochemical study. Am J Surg Pathol 1993;17:706–14.
2. Sircar K, Hewlett BR, Huizinga JD, Chorneyko K, Berezin I, Riddell RH. Interstitial cells of Cajal as precursors of gastrointestinal stromal tumors. Am J Surg Pathol 1999;23:377–89.
3. Kindblom LG, Remotti HE, Aldenborg F, Meis-Kindblom JM. Gastrointestinal pacemaker cell tumor (GIPACT): gastrointestinal stromal tumors show phenotypic characteristics of the interstitial cells of Cajal. Am J Pathol 1998;152:1259–69.
4. Reddy RM, Fleshman JW. Colorectal gastrointestinal stromal tumors: a brief review. Clin Colon Rectal Surg 2006;19:69–77.
5. Ding G, Yang J, Cheng S, Kai L, Nan L, Zhang S, et al. A rare case of rapid growth of exophytic gastrointestinal stromal tumor of the stomach. Dig Dis Sci 2005;50:820–3.
6. Otani Y, Furukawa T, Yoshida M, Saikawa Y, Wada N, Ueda M, et al. Operative indications for relatively small (2–5 cm) gastrointestinal stromal tumor of the stomach based on analysis of 60 operated cases. Surgery 2006;139:484–92.
7. Tanaka J, Oshima T, Hori K, Tomita T, Kim Y, Watari J, et al. Small gastrointestinal stromal tumor of the stomach showing

rapid growth and early metastasis to the liver. Dig Endosc 2010; 22:354–6.
8. Demetri GD, Benjamin RS, Blanke CD, Blay JY, Casali P, Choi H, et al. NCCN Task Force report: management of patients with gastrointestinal stromal tumor (GIST)–update of the NCCN clinical practice guidelines. J Natl Compr Canc Netw 2007;5 Suppl 2:S1–29; quiz S30.
9. Dolmans DE, Fukumura D, Jain RK. Photodynamic therapy for cancer. Nat Rev Cancer 2003;3:380–7.
10. Juarranz A, Jaen P, Sanz-Rodriguez F, Cuevas J, Gonzalez S. Photodynamic therapy of cancer: basic principles and applications. Clin Transl Oncol 2008;10:148–54.
11. Triesscheijn M, Baas P, Schellens JH, Stewart FA. Photodynamic therapy in oncology. Oncologist 2006;11:1034–44.
12. Detty MR, Gibson SL, Wagner SJ. Current clinical and preclinical photosensitizers for use in photodynamic therapy. J Med Chem 2004;47:3897–915.
13. Gomer CJ, Ferrario A. Tissue distribution and photosensitizing properties of mono-L-aspartyl chlorin e6 in a mouse tumor model. Cancer Res 1990;50:3985–90.
14. Kato H, Furukawa K, Sato M, Okunaka T, Kusunoki Y, Kawahara M, et al. Phase II clinical study of photodynamic therapy using mono-L-aspartyl chlorin e6 and diode laser for early superficial squamous cell carcinoma of the lung. Lung Cancer 2003;42:103–11.
15. Kujundzic M, Vogl TJ, Stimac D, Rustemovic N, Hsi RA, Roh M, et al. A Phase II safety and effect on time to tumor progression study of intratumoral light infusion technology using talaporfin sodium in patients with metastatic colorectal cancer. J Surg Oncol 2007;96:518–24.
16. Tanaka M, Kataoka H, Mabuchi M, Sakuma S, Takahashi S, Tujii R, et al. Anticancer effects of novel photodynamic therapy with glyco-conjugated chlorin for gastric and colon cancer. Anticancer Res 2011;31:763–9.
17. Taguchi T, Sonobe H, Toyonaga S, Yamasaki I, Shuin T, Takano A, et al. Conventional and molecular cytogenetic characterization of a new human cell line, GIST-T1, established from gastrointestinal stromal tumor. Lab Invest 2002;82:663–5.
18. Zou C, Wang Y, Shen Z. 2-NBDG as a fluorescent indicator for direct glucose uptake measurement. J Biochem Biophys Methods 2005; 64:207–15.
19. Hirota S, Isozaki K, Moriyama Y, Hashimoto K, Nishida T, Ishiguro S, et al. Gain-of-function mutations of c-kit in human gastrointestinal stromal tumors. Science 1998;279:577–80.
20. Hirohara S, Obata M, Ogata S, Kajiwara K, Ohtsuki C, Tanihara M, et al. Sugar-dependent aggregation of glycoconjugated chlorins and its effect on photocytotoxicity in HeLa cells. J Photochem Photobiol B 2006;84:56–63.
21. Hirohara S, Obata M, Alitomo H, Sharyo K, Ando T, Tanihara M, et al. Synthesis, photophysical properties and sugar-dependent *in vitro* photocytotoxicity of pyrrolidine-fused chlorins bearing S-glycosides. J Photochem Photobiol B 2009;97:22–33.
22. Yano S, Hirohara S, Obata M, Hagiya Y, Ogura S, Ikeda A, et al. Current states and future views in photodynamic therapy. J Photochem Photobiol C 2011;12:46–67.
23. Bisland SK, Singh D, Gariepy J. Potentiation of chlorin e6 photodynamic activity *in vitro* with peptide-based intracellular vehicles. Bioconjug Chem 1999;10:982–92.
24. Del Governatore M, Hamblin MR, Shea CR, Rizvi I, Molpus KG, Tanabe KK, et al. Experimental photoimmunotherapy of hepatic metastases of colorectal cancer with a 17.1A chlorin(e6) immunoconjugate. Cancer Res 2000;60:4200–5.
25. Sharman WM, van Lier JE, Allen CM. Targeted photodynamic therapy via receptor mediated delivery systems. Adv Drug Deliv Rev 2004;56:53–76.
26. Chen B, Pogue BW, Hasan T. Liposomal delivery of photosensitising agents. Expert Opin Drug Deliv 2005;2:477–87.
27. Ichikawa K, Hikita T, Maeda N, Yonezawa S, Takeuchi Y, Asai T, et al. Antiangiogenic photodynamic therapy (PDT) by using long-circulating liposomes modified with peptide specific to angiogenic vessels. Biochim Biophys Acta 2005;1669:69–74.
28. Konan YN, Berton M, Gurny R, Allemann E. Enhanced photodynamic activity of meso-tetra(4-hydroxyphenyl)porphyrin by incorporation into sub-200 nm nanoparticles. Eur J Pharm Sci 2003;18:241–9.
29. Loo C, Lowery A, Halas N, West J, Drezek R. Immunotargeted nanoshells for integrated cancer imaging and therapy. Nano Lett 2005;5:709–11.
30. Reddy GR, Bhojani MS, McConville P, Moody J, Moffat BA, Hall DE, et al. Vascular targeted nanoparticles for imaging and treatment of brain tumors. Clin Cancer Res 2006;12:6677–86.
31. Zhao B, Yin JJ, Bilski PJ, Chignell CF, Roberts JE, He YY. Enhanced photodynamic efficacy towards melanoma cells by encapsulation of Pc4 in silica nanoparticles. Toxicol Appl Pharmacol 2009;241:163–72.
32. Manolescu AR, Witkowska K, Kinnaird A, Cessford T, Cheeseman C. Facilitated hexose transporters: new perspectives on form and function. Physiology (Bethesda) 2007;22:234–40.
33. Zhao FQ, Keating AF. Functional properties and genomics of glucose transporters. Curr Genomics 2007;8:113–28.
34. Young CD, Lewis AS, Rudolph MC, Ruehle MD, Jackman MR, Yun UJ, et al. Modulation of glucose transporter 1 (GLUT1) expression levels alters mouse mammary tumor cell growth in vitro and in vivo. PLoS ONE 2011;6:e23205.
35. Younes M, Brown RW, Stephenson M, Gondo M, Cagle PT. Overexpression of Glut1 and Glut3 in stage I nonsmall cell lung carcinoma is associated with poor survival. Cancer 1997;80:1046–51.
36. Kang SS, Chun YK, Hur MH, Lee HK, Kim YJ, Hong SR, et al. Clinical significance of glucose transporter 1 (GLUT1) expression in human breast carcinoma. Jpn J Cancer Res 2002;93:1123–8.
37. Amann T, Maegdefrau U, Hartmann A, Agaimy A, Marienhagen J, Weiss TS, et al. GLUT1 expression is increased in hepatocellular carcinoma and promotes tumorigenesis. Am J Pathol 2009;174:1544–52.
38. Reske SN, Grillenberger KG, Glatting G, Port M, Hildebrandt M, Gansauge F, et al. Overexpression of glucose transporter 1 and increased FDG uptake in pancreatic carcinoma. J Nucl Med 1997;38:1344–8.
39. Bos R, van Der Hoeven JJ, van Der Wall E, van Der Groep P, van Diest PJ, Comans EF, et al. Biologic correlates of (18)fluorodeoxyglucose uptake in human breast cancer measured by positron emission tomography. J Clin Oncol 2002;20:379–87.
40. Hiyoshi Y, Watanabe M, Imamura Y, Nagai Y, Baba Y, Yoshida N, et al. The relationship between the glucose transporter type 1 expression and F-fluorodeoxyglucose uptake in esophageal squamous cell carcinoma. Oncology 2009;76:286–92.
41. Cullinane C, Dorow DS, Kansara M, Conus N, Binns D, Hicks RJ, et al. An *in vivo* tumor model exploiting metabolic response as a biomarker for targeted drug development. Cancer Res 2005;65:9633–6.
42. Yun J, Rago C, Cheong I, Pagliarini R, Angenendt P, Rajagopalan H, et al. Glucose deprivation contributes to the development of KRAS pathway mutations in tumor cells. Science 2009;325:1555–9.
43. Kawamura A, Adachi K, Ishihara S, Katsube T, Takashima T, Yuki M, et al. Correlation between microsatellite instability and metachronous disease recurrence after endoscopic mucosal resection in patients with early stage gastric carcinoma. Cancer 2001;91:339–45.
44. Yamada A, Oguchi K, Fukushima M, Imai Y, Kadoya M. Evaluation of 2-deoxy-2-[18F]fluoro-D-glucose positron emission tomography in gastric carcinoma: relation to histological subtypes, depth of tumor invasion, and glucose transporter-1 expression. Ann Nucl Med 2006; 20:597–604.
45. Chung HW, Lee SY, Han HS, Park HS, Yang JH, Lee HH, et al. Gastric cancers with microsatellite instability exhibit high fluorodeoxyglucose uptake on positron emission tomography. Gastric Cancer 2013; 16:185–92.
46. Buytaert E, Dewaele M, Agostinis P. Molecular effectors of multiple cell death pathways initiated by photodynamic therapy. Biochim Biophys Acta 2007;1776:86–107.
47. Peng Q, Warloe T, Moan J, Godal A, Apricena F, Giercksky KE, et al. Antitumor effect of 5-aminolevulinic acid-mediated photodynamic therapy can be enhanced by the use of a low dose of photofrin in human tumor xenografts. Cancer Res 2001;61:5824–32.
48. Schastak S, Jean B, Handzel R, Kostenich G, Hermann R, Sack U, et al. Improved pharmacokinetics, biodistribution and necrosis *in vivo* using a new near infra-red photosensitizer: tetrahydroporphyrin tetratosylat. J Photochem Photobiol B 2005;78:203–13.
49. Lim YC, Yoo JO, Park D, Kang G, Hwang BM, Kim YM, et al. Antitumor effect of photodynamic therapy with chlorin-based photosensitizer DH-II-24 in colorectal carcinoma. Cancer Sci 2009;100:2431–6.